

ELASTIC ANISOTROPY OF Zr-2.5%Nb ALLOY CANDU PRESSURE TUBE BY ULTRASONIC METHODS

V. IONESCU, M. MIHALACHE, S. FLOREA

Institute for Nuclear Research, Pitesti, Romania
E-mail: viorel.ionescu@nuclear.ro

Received October 16, 2009

Abstract. In the present paper, the hydrogen influence on the acousto-elastic properties of Zr-2.5%Nb alloy will be investigated using non-destructive method, based on measurements of ultrasonic velocity. In order to obtain the most usual elastic coefficients on a given direction (axial, circumferential and radial) of the tube, both longitudinal V_L and transversal V_T phase velocities have been experimentally determined.

Key words: zirconium hydride, elastic modulus, ultrasonic methods.

1. INTRODUCTION

The cold-worked Zr-2.5%Nb alloy is used as material for the pressure tubes of CANDU nuclear reactors. It has developed a strong texture due to the limited slip system during extrusion process, leading to anisotropic properties [1]. The material properties are strongly dependent on the orientation distributions of grains. For these reasons a directional anisotropy of elastic coefficients results.

During the service life in reactor, diffusion of hydrogen and/or deuterium in the pressure tubes wall may occur [2]. Hydrogen has very limited solubility in zirconium alloys; when the hydrogen concentration exceeds Terminal Solid Solubility (TSS), a brittle second phase (hydrides) appears.

The hydrides preferentially precipitate along the grain boundaries and even in small concentrations, can potentially have a dramatic effect on the structural integrity of zirconium alloys nuclear components.

To characterize the degree of anisotropy and the hydrogen influence, it is necessary to determine the anisotropic elastic modulus on the main directions (axial, circumferential and radial) of the tube samples.

2. EXPERIMENTAL PROCEDURE

2.1. Elastic Modulus

The anisotropy of the Zr-2.5%Nb alloy could be considered as an orthorhombic symmetry, with three principal directions such as radial, transversal and longitudinal directions.

Ultrasonic velocity can be related to elastic properties and mechanical relaxation processes. The most usual elastic coefficients may be expressed from the propagation equations of the ultrasonic waves [3-8], as follows:

$$E = \rho \cdot v_T^2 \frac{(3v_L^2 - 4v_T^2)}{(v_L^2 - v_T^2)} \quad \text{Young modulus,} \quad (1)$$

$$G = \rho \cdot v_T^2 \quad \text{shear modulus,} \quad (2)$$

$$\nu = \frac{v_L^2 - 2v_T^2}{2(v_L^2 - v_T^2)} \quad \text{Poisson ratio,} \quad (3)$$

$$K = \rho \left(v_L^2 - \frac{4v_T^2}{3} \right) \quad \text{compressibility modulus,} \quad (4)$$

where ρ is the material density.

In order to obtain these elastic coefficients (Equations 1 to 4) on a given direction, both longitudinal, V_L , and transversal, V_T , phase velocities have been experimentally determined by length and ultrasonic time of flight measurements.

2.2. Specimen Preparation

The measurements were performed at room temperature using a set of samples (A1÷A12) from the same as received Zr-2.5%wtNb tube, at 30° angular increment in the circumferential-radial plane. Each sample was machined to a rectangular parallelepiped form, in order to measure the length and the ultrasonic time of flight, and to determine the phase velocity on the following directions of the pressure tube: axial (A), circumferential (C) and radial (R).

This material has a hexagonal closed packed (hcp) structure, textured along the circumferential direction (the effective fraction of cells having the \vec{C} axis oriented around the circumferential direction of the tube). The orientation distribution of grains in circumferential-radial section is the circumferential direction of the tube. A typical digital microscopy image of Zr-2.5%Nb pressure tube materials is shown in Fig. 1.

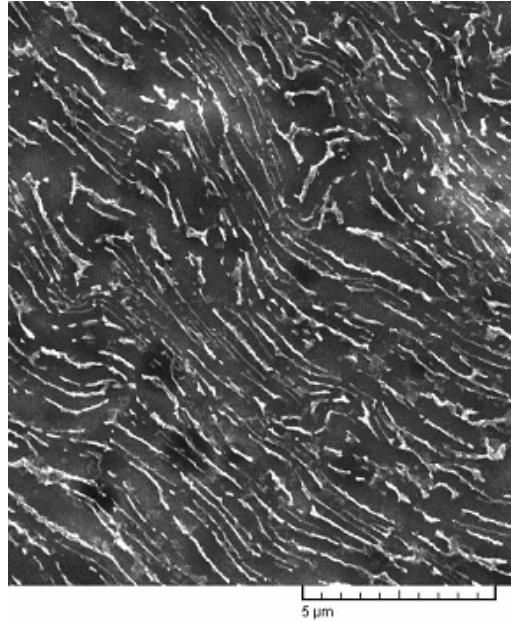


Fig. 1 – SEM image of Zr-2.5%Nb showing the grains limits in radial-circumferential section.

2.3. Experimental System

The time of flight was measured by pulse-echo technique. The technique requires an ultrasonic pulser-receiver (USIP12/KRAUTKRAMER instrument equipped with the special module DTM12), a longitudinal transducer (ALPHA HP AEROTECH – 10 MHz /.25 miniature broadband) and a shear wave contact transducer (V156 – 5MHz normal incidence).

3. EXPERIMENTAL RESULTS AND DISCUSSIONS

The averaged values of longitudinal phase velocity obtained on the samples, in the “as received” state, are: $V_C = 4.799\text{mm}/\mu\text{s}$, $V_A = 4.680\text{mm}/\mu\text{s}$, $V_R = 4.707\text{mm}/\mu\text{s}$. It can be seen that the smallest values correspond to the axial direction and the larger one to the circumferential direction.

For these measurements, performed at same conditions it was determined the sample standard deviation:

$$s = \sqrt{\frac{1}{n-1} \sum_{i=1}^n (x_i - \bar{x})^2}, \quad (5)$$

where: n = number of measurements; x_i = the measured values; \bar{x} = the mean value of measured values.

After the initial phase velocities measurements, one set of samples (A1÷A6) was hydrided by slow-rate electrolytic reaction, and the other (A7÷A12) was hydrided by fast plasma process. The samples were hydrided at different hydrogen concentrations: A1(55ppm), A2(65ppm), A3(90ppm), A4(110ppm), A5(125ppm), A6(155ppm), A7(78ppm), A8(100ppm), A9(112ppm), A10(119ppm), A11(141ppm), A12(158ppm). The samples hydrogen content characterization is performed by an ELTRA 04-900 analyser, based on the inert fusion method. The method accuracy is ± 5 ppm H_2 .

The metallographic study of hydrided samples (Fig. 2) shows the following:

- ◆ the electrolytic hydrided samples (Fig. 2a) contain δ hydrides platelets especially which form relatively long “filaments” with prevalent orientation in the circumferential direction;
- ◆ the orientation of hydride precipitates within the pressure tube samples is dependent upon the tube texture and stress state. Most of the hydrides are oriented in the circumferential direction of the tube due to the preferred crystallographic orientation of the tube (Fig. 1);
- ◆ the length of the δ filaments is larger at high values of hydrogen concentration C_H (from about $20\mu m$ at $C_H \cong 40ppm$ to about $300\mu m$ for $C_H \cong 160ppm$). The distance between the filaments decrease from approx. $200\mu m$ at $C_H \cong 40ppm$, to approx. $50\mu m$ for $C_H \cong 160ppm$;
- ◆ in the case of the plasma hydrided samples (Fig. 2b), the fraction of γ hydrides (the small dark points) is significantly increased. As a consequence, at comparable hydrogen concentration a smaller number of δ hydride filaments can be put into the evidence, with a significant greater distance between them.

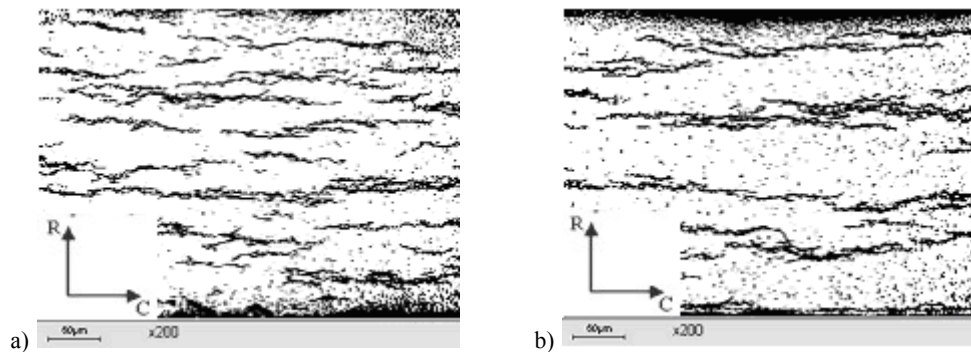


Fig. 2 – Optical light micrography – methalographic images of hydrides;
a) $C_H=120ppm$ (electrolytic), b) $C_H=110ppm$ (plasma).

After the hydriding process, the longitudinal and shear phase velocities were determined again, on these samples. The experimental points united by guiding lines were graphically represented in Figs. 3 and 4, and it can be seen that the investigated Zr-2.5%Nb alloy preserve a very pronounced acoustic anisotropy.

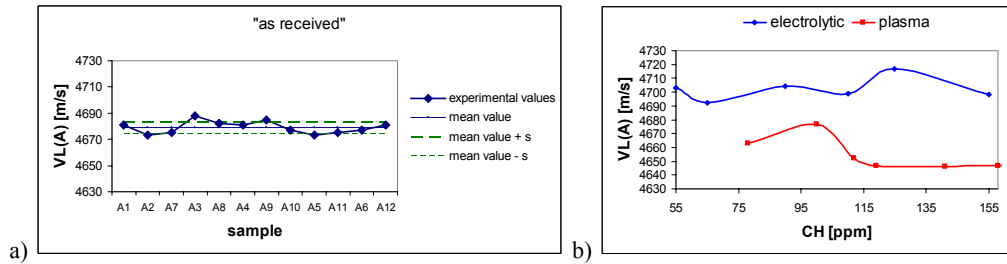


Fig. 3 – Longitudinal velocity on axial direction: a) “as received” material; b) hydrided material at different hydrogen concentrations.

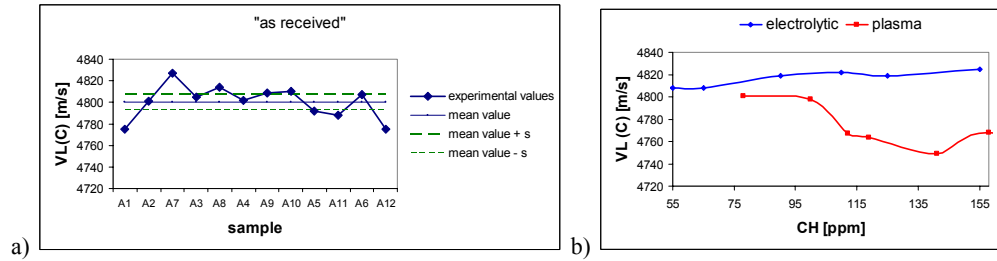


Fig. 4 – Longitudinal velocity on circumferential direction: a) “as received” material; b) hydrided material at different hydrogen concentrations.

Measurements of the longitudinal phase velocity and the graphic representations of these data have shown a completely different behaviour between slow-rate hydrided (A1÷A6) and fast hydrided (A7÷A12) samples.

In the case of slow-rate hydrided samples, by electrolytic reaction, the longitudinal velocity is slightly increased as a function of the hydrogen concentration C_H . Contrary, in the case of fast hydrided samples by metal-hydrogen plasma interaction process, a decrease of the longitudinal velocity with the hydrogen concentration, can be observed.

A possible explanation of this difference, in the material behaviour, could be the influence of the high level internal stresses, developed by the fast hydrogen precipitation, known that the longitudinal velocity in zirconium alloys decreases by increasing the mechanical stresses.

The data measured with this method are used to calculate the values of Poisson coefficients ν , Young modulus E , shear modulus G , compressibility modulus (Equations 1 to 4).

The dependencies of these elastic modulus on the hydrogen concentration C_H are graphically represented (Figs. 5b to 12b). The determined points are united by guiding lines.

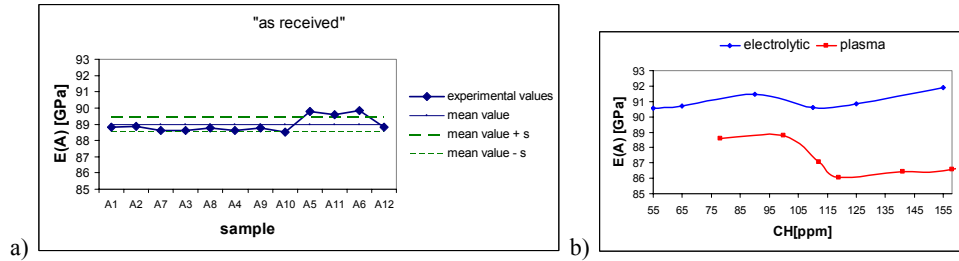


Fig. 5 – Young modulus on axial direction: a) “as received” material; b) hydrided material at different hydrogen concentrations.

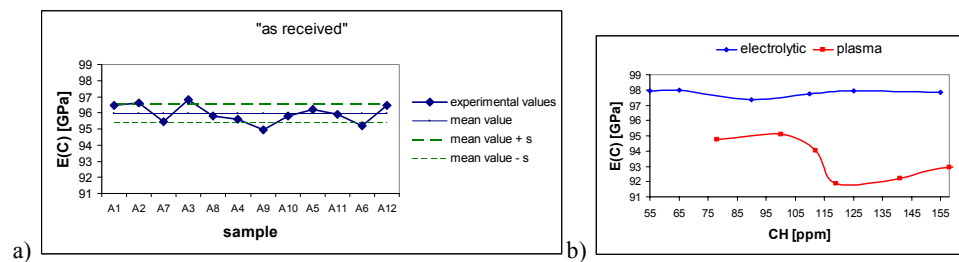


Fig. 6 – Young modulus on circumferential direction: a) “as received” material; b) hydrided material at different hydrogen concentrations.

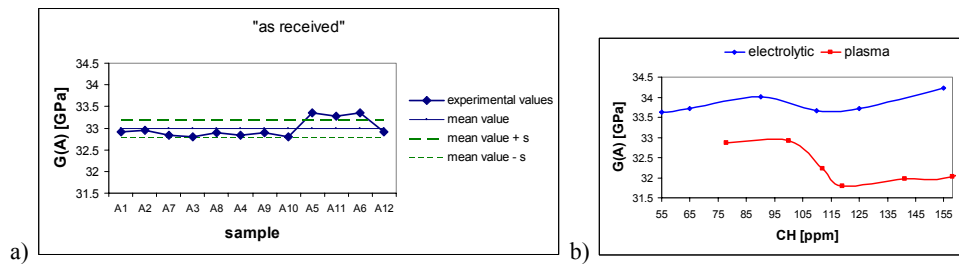


Fig. 7 – Shear modulus on axial direction: a) “as received” material; b) hydrided material at different hydrogen concentrations.

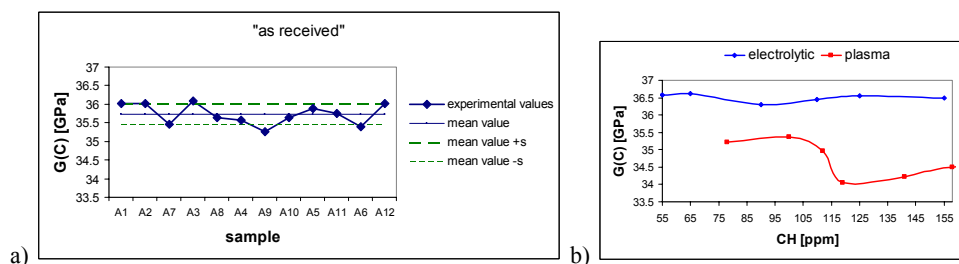


Fig. 8 – Shear modulus on circumferential direction: a) “as received” material; b) hydrided material at different hydrogen concentrations.

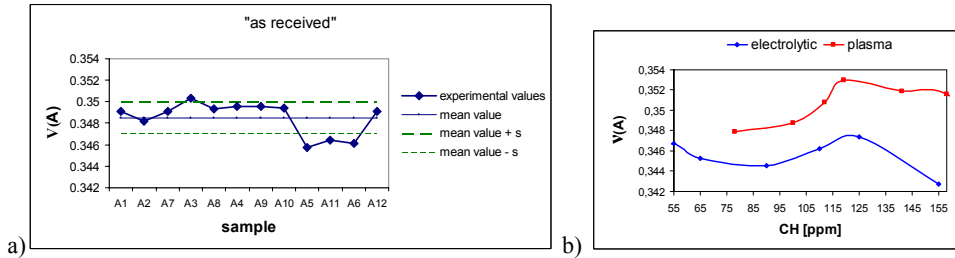


Fig. 9 – Poisson coefficients on axial direction: a) “as received” material; b) hydrided material at different hydrogen concentrations.

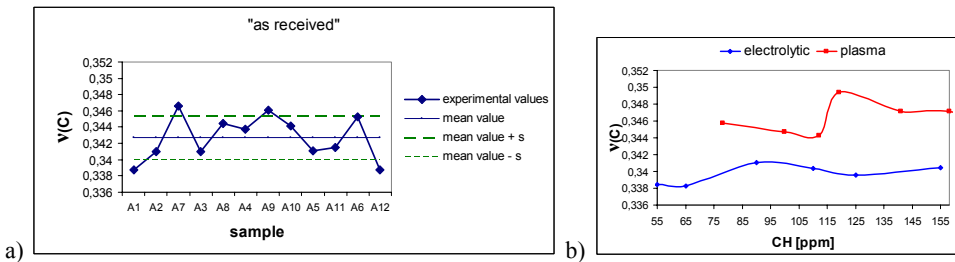


Fig. 10 – Poisson coefficients on circumferential direction: a) “as received” material; b) hydrided material at different hydrogen concentrations.

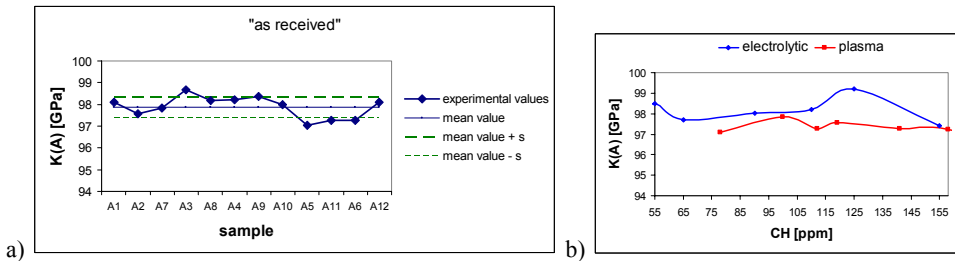


Fig. 11 – Compressibility modulus on axial direction: a) “as received” material; b) hydrided material at different hydrogen concentrations.

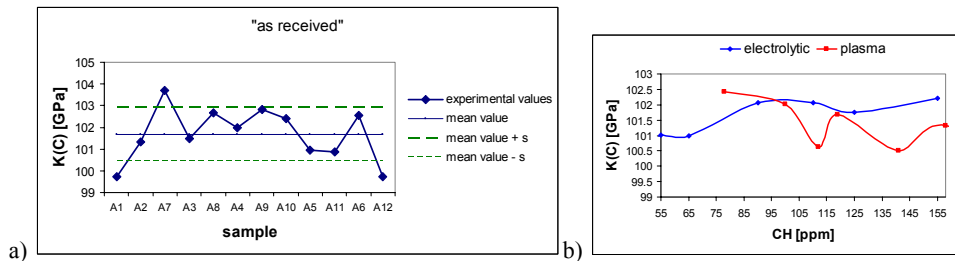


Fig. 12 – Compressibility modulus on circumferential direction: a) “as received” material; b) hydrided material at different hydrogen concentrations.

By polynomial regression, the semi-empirical laws (Table 1) can be obtained, which establish a correlation between elastic modulus and hydrogen content, based on ultrasonic measurements.

These are very useful for the numerical simulation of the pressure tube behaviour.

It is important to note the good agreement between our measured values, for the ultrasonic phase velocity and the already published data [9].

Table 1

The polynomial expressions for hydrogen concentration C_H [ppm] dependence of elastic constants at room temperature

| direction | hydriding process | polynomial expressions for: E[GPa]; G[GPa]; ν ; K[GPa] |
|-----------|-------------------|---|
| A | plasma | $E(x) = 2E-05x^2 - 9.3E-03x + 88.379$ |
| A | electrolytic | $E(x) = -4E-06x^2 + 8.5E-03x + 90.280$ |
| C | plasma | $E(x) = 7E-05x^2 - 3.3E-02x + 96.518$ |
| C | electrolytic | $E(x) = -7E-05x^2 + 1.2E-02x + 97.480$ |
| A | plasma | $G(x) = 5E-06x^2 - 3.1E-03x + 32.701$ |
| A | electrolytic | $G(x) = 3E-06x^2 + 0.2.6E-03x + 33.562$ |
| C | plasma | $G(x) = 3E-05x^2 - 1.3E-02x + 35.876$ |
| C | electrolytic | $G(x) = -3E-05x^2 + 4E-03x + 36.438$ |
| A | plasma | $\nu(x) = 3E-08x^2 - 1E-05x + 0.351$ |
| A | electrolytic | $\nu(x) = -2E-07x^2 + 2E-05x + 0.345$ |
| C | plasma | $\nu(x) = -3E-08x^2 + 1E-05x + 0.345$ |
| C | electrolytic | $\nu(x) = 6E-08x^2 + 1E-05x + 0.337$ |
| A | plasma | $K(x) = 4E-05x^2 - 1.9E-02x + 98.913$ |
| A | electrolytic | $K(x) = -1E-04x^2 + 2.2E-02x + 97.082$ |
| C | plasma | $K(x) = 5E-05x^2 - 2.7E-02x + 103.790$ |
| C | electrolytic | $K(x) = -3E-05x^2 + 1.9E-02x + 100.040$ |

Notation: x = hydrogen concentration C_H [ppm]; A = axial direction; C = circumferential direction.

4. CONCLUSIONS

The smallest values of longitudinal and transversal phase velocity obtained in both “as received” and hydrided state, correspond to the axial direction and the highest to the circumferential direction. For polycrystalline zirconium, the wave velocity is dependent on the effective fraction of cells having the \bar{C} axis aligned with the wave vector. Thus, it can be deduced that in the Zr-2.5%Nb pressure tube the most part of α -Zr grains (hcp crystallographic structure) have the \bar{C} axis oriented around the circumferential direction of the tube. This is in accordance with the texture required in the pressure tube manufacturing specification [10÷12].

The study of the hydrogen effect, on the acousto-elastic properties of Zr-2.5%Nb alloy, using ultrasonic methods, have shown a different dependence of the ultrasonic velocities and elastic moduli on the hydrogen concentration for the slow-rate hydrided samples and for the fast hydrided ones.

An explanation of this difference, in the behaviour, can be explained due to the high level internal stresses developed in the case of fast hydrogen precipitation. The study has shown a different elastically behaviour between axial (A) and circumferential (C) directions.

Semiempirical relationships for Zr-2.5%Nb alloy were obtained, as correlations between elastic modulus and hydrogen concentration, based on ultrasonic measurements.

The further study of this experimental results is important, in order to elaborate a nondestructive method for determination of hydrogen content into Zr alloys.

REFERENCES

1. D. Ciurchea, *Texture induced anisotropy in zircaloy-4 tubes*, Journal of Nuclear Materials, **131**, 1, 1–10, (1985).
2. R.N. Singh, R. Kishorea, S.S. Singh, T.K. Sinha, B.P. Kashyap, *Stress-reorientation of hydrides and hydride embrittlement of Zr-2.5 wt% Nb pressure tube alloy*, Journal of Nuclear Materials, **325** (2004).
3. Joseph L. Rose, *Ultrasonic waves in solid media*, Cambridge University Press, 2006.
4. Rohn Truell, *Ultrasonic methods in Solid State Physics*, Academic Press-New.
5. Fedor I. Fedorov, *Theory of Elastic Waves in Crystals*, Plenum Press, New York (1968).
6. Y.-M. Cheong, *Determination of anisotropic elastic moduli of Zr-2.5%Nb CANDU pressure tube materials*, Journal of Materials Science, **35**, 1195–1200 (2000).
7. D.O. Northwood, *Elastic Constants of Zirconium Alloys*, Journal of Nuclear Materials, **55**, 299–310 (1975).
8. Charles Kittel, *Fizica corpului solid*, Edit. Tehnică, București, York, London, 1969.
9. M. Soare, C. Iordache, *Ultrasonic Critical Angle Spectroscopy: a powerful method for acousto-elastic characterization of materials* (COG/IAEA Technical Meeting, Argentina, April 1997).
10. Takao Konishi, Masahiro Honji, *Texture Effect of Zircaloy on Ultrasonic Velocity*, 6th International Conference on Zirconium in the Nuclear Industry, Vancouver, Canada, 1982.
11. *** CAN/CSA-N285.6.7-88 Standard Zirconium Alloy Design Data.
12. *** AECL Technical Specification TS-XX-31110-5/78-06-08 Cold worked Zirconium-2.5% Niobium extruded and drawn pressure tubes.